

PACS numbers: 42.55.Lt; 24.90.+d; 42.87.Bg
DOI: 10.1070/QE2001v031n06ABEH001988

Interferometric technique for determining the energy deposition in gas-flow nuclear-pumped lasers

A A Pikulev

***Abstract*. An interference technique is developed for determining the energy deposition in gas-flow lasers pumped by uranium fission fragments. It is shown that four types of interference patterns may be formed. Algorithms are presented for determining the type of interference and for enumerating the maxima in interference pattern.**

Keywords: *interference, output parameters of lasers, nuclear-pumped lasers.*

1. Introduction

Detailed studies of the energy deposition in the active medium are necessary for creating powerful cw lasers pumped by the fission fragments of uranium [1]. A knowledge of the energy deposition is required for determining important parameters such as the efficiency of a laser, temperature of the working medium, stability of the resonator, optical property of the laser beam, etc. Usually, the energy deposition is determined by two methods: the method of pressure drop in the sealed cells of nuclear-pumped lasers (NPLs) [2 – 4], and the method of thin wires used both for gas-flow channels and for sealed channels in lasers [5].

The first method can be used for determining only the average energy deposition, and the second one for determining the energy deposition distribution over the channel volume. Note that the method of thin wires yields not the energy deposition, but rather the total energy flux transported by the fission fragments, so that the energy deposition can be determined only if the density of the gas is known at each point.

In addition to these two methods of determining the energy deposition, one can also use the interferometric experiments, which were earlier carried out for determining the optical inhomogeneities emerging both in the sealed [6] and in gas-flow channels [7, 8] of NPLs. The density and temperature of the gas, and hence the energy deposited in it, can be determined directly from the interference patterns. The experiments [7, 8] were performed using the gas-flow setup with plane uranium layers, which is a prototype of the LM-4 working laser setup [9]. Note that because the pulse duration of the VIR-2M reactor used for pumping was about of 3 ms [10], the thermodynamic processes in these experiments were transient and the results obtained in Refs [7, 8] cannot be generalised directly to the case of cw gas-flow NPLs, although the main features of the thermodynamics of gas-flow channels of NPLs are preserved.

The aim of this paper is to develop the method for determining the energy deposition in the gas-flow channels of NPLs from the results of interferometric measurements. This method comprises two stages: the processing of interference patterns and the computation of the energy deposition. The main purpose of the first stage is to enumerate the maxima in the interference pattern. In the case of bulk energy deposition, the solution of this problem requires a certain 'qualitative' information on the distribution of the energy deposition over the volume of the laser channel. It is shown that four types of interference patterns are possible, and an algorithm is presented for identifying the type of interference patterns.

The second stage is directly related to the gasdynamic and thermodynamic processes occurring in the NPL channels. The energy deposition was calculated using the model of rectilinear current lines disregarding the wall effects and heat conduction. This model is the simplest among the models of the gas dynamics of gas-flow channels, and the obtained solution can be used, if required, as a first approximation in more precise models.

2. Basic equations

Consider the thermodynamics of a gas in the gas-flow channels of an NPL. We assume that the gas flows under a constant pressure. The heat conduction in the wall region and in the wake of the radiator is neglected. In this case, the equations of energy conservation and continuity have the form [11, 12]

$$c_p\rho\left(\frac{\partial T}{\partial t}+\boldsymbol{U}\nabla T\right)=q,\quad \frac{\partial\rho}{\partial t}+\boldsymbol{U}\nabla\rho=0, \tag{1}$$

where $\rho, \boldsymbol{U}, T$ are the density, velocity and temperature of the gas; c_p is the specific heat of the gas at constant pressure; and q is the bulk energy deposition. In addition to Eqns (1), the gas flow should be described by the Navier – Stokes or Euler equations [12]. Fig. 1 shows a schematic of the gas-flow channel (the second radiator is not shown).

A A Pikulev All-Russian Federal Nuclear Centre, All-Russian Research Institute of Experimental Physics, ul. Mira, 37, 607190 Sarov, Nizhegorodskaya oblast, Russia; tel.: (83130) 1 11 51

Received 19 October 2000, revision received 19 February 2001
Kvantovaya Elektronika **31** (6) 500 – 504 (2001)
Translated by Ram Wadhwa

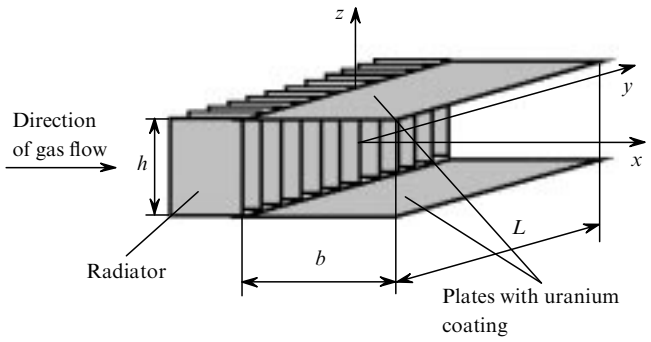

Figure 1. Schematic of the gas-flow channel.

The gas flux at the channel input has a velocity U_0, density ρ_0, and temperature T_0.

Assuming that the current lines are rectilinear and parallel to the x axis in the case of a steady-state flow, Eqns (1) can be simplified:

$$\frac{\partial \Delta T}{\partial x} = \frac{q}{c_p \rho_0 U_0}, \quad \rho U = \rho_0 U_0 = \text{const}, \tag{2}$$

where $\Delta T = T - T_0$ is the increment in the gas temperature. One can see from Eqn (2) that in the case of a steady-state process, the knowledge of the temperature distribution in the channel is sufficient for finding the energy deposition distribution.

For an ideal gas under a constant pressure, the change in the refractive index is related to temperature by the familiar expression [13]

$$\Delta n = -\frac{(n_0 - 1)}{T_0 + \Delta T} \Delta T, \tag{3}$$

where n_0 is the refractive index of the gas at temperature T_0. The additional phase incursion in the measuring channel is

$$\varphi = k \int_0^L \Delta n \, \mathrm{d}y = -k(n_0 - 1) \int_0^L \frac{\Delta T}{T_0 + \Delta T} \, \mathrm{d}y, \tag{4}$$

where k is the wave number and L is the channel length.

Fig. 2 shows the scheme of interferometric measurements using a Mach–Zehnder interferometer [14]. A parallel laser beam is split into two beams, one of the beams passing through the measuring channel and the other through the reference channel. The introduction of an optical wedge in the reference channel facilitates the measurements. The intensities of both the beams are assumed to be identical. In this case, the contrast of the interference pattern is the sharpest. The interference maxima satisfy the equation [13]

$$\varphi(x_m(z), z) + 2\pi N x_m(z) = 2\pi m + \varphi_0, \tag{5}$$

where N is the number of interference fringes per unit length; φ_0 is the initial phase difference ($0 \leqslant \varphi_0 < 2\pi$); $x_m(z)$ is the position of the mth maximum. In the absence of heating, the interference maxima represent equidistant straight lines parallel to z axis. The position of these lines is defined by the formula

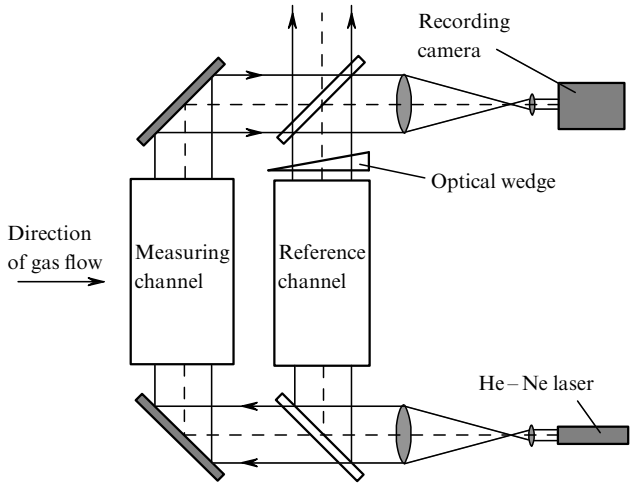

Figure 2. Schematic of the Mach–Zehnder interferometer.

$$2\pi N \Delta_m = 2\pi m + \varphi_0, \quad \varphi_0 = 2\pi N \Delta_0, \tag{6}$$

where Δ_m is the unperturbed position of the mth maximum.

3. Interferometry of gas-flow lasers

Consider the interference pattern of the gas-flow channel of an NPL. Note that the integrand in formula (4) cannot be taken out of the integral sign because of the nonuniformity of the energy deposition distribution along the optical axis y of the channel [15]. Because ΔT is a continuous function of the coordinate y, we can apply the mean-value theorem to Eqn (4) [16]:

$$\int_0^L \frac{\Delta T}{T_0 + \Delta T} \, \mathrm{d}y = \frac{L \Delta T^*}{T_0 + \Delta T^*}, \tag{7}$$

where $\Delta T^* \equiv \Delta T(y^*); y^* \in [0, L]$.

This means that the interference pattern can be treated as the result of an averaging of the function ΔT along the y axis. Knowing the distribution of the energy deposition q along the coordinate y, we can establish a one-to-one correspondence between the functions ΔT and ΔT^*.

Taking into account Eqns (4) and (7), we can present Eqn (5) in the form

$$N x_m(z) - \frac{\varphi_0}{2\pi} - m = \frac{kL(n_0 - 1)}{2\pi} \frac{\Delta T^*}{T_0 + \Delta T^*}. \tag{8}$$

The number of solutions of this equation depends on the parameters N and m. To study the graphic solution of this equation, we fix the coordinate z and consider the left- and right-hand sides of Eqn (8) for different m. We introduce the notation

$$\begin{aligned} a(x) &= Nx - \frac{\varphi_0}{2\pi} - m, \\ g(x, z) &= \frac{kL(n_0 - 1)}{2\pi} \frac{\Delta T^*(x, z)}{T_0 + \Delta T^*(x, z)}. \end{aligned} \tag{9}$$

The function a defines a family of straight lines with the slope N. Consider the behaviour of the function g. For $z =$ const, the function ΔT^* is a monotonically increasing function, and $\Delta T^* \sim x$ for small x [17]. Fig. 3 shows functions a

(for $N > 0$) and g. One can see that the number of solutions of equation $a(x) = g(x)$ may be two, one or zero for each value of the parameter m. For $m \leqslant 0, N > 0$ the number of solutions may be two or zero. Only one solution exists for $m > 0, N > 0$. For $N \leqslant 0$, a solution exists only for $m \leqslant 0$.

All solutions of Eqn (8) for $z = \text{const}$ can be divided into two classes. This is illustrated in Fig. 3 showing three functions which satisfy the condition $g_1 \leqslant g_2 \leqslant g_3$. One can see that there are two types of solutions exhibiting different behaviour upon a variation of the function g:

(1) Solutions that are displaced towards the origin of coordinates with increasing g and away from the origin with decreasing g. Such solutions will be called A-points.

(2) Solutions that are displaced away from the origin of coordinates with increasing g and towards the origin with decreasing g. Such solutions will be called B-points.

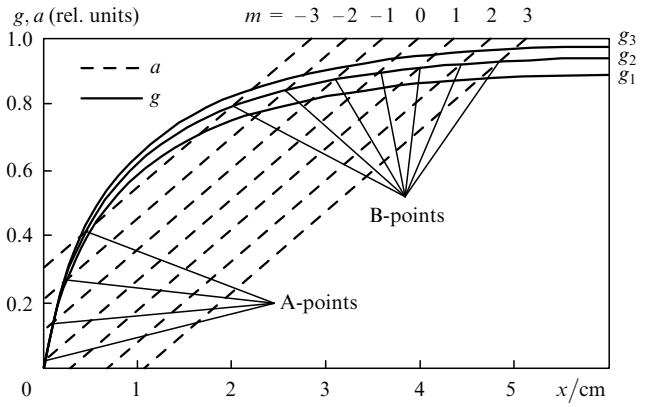

Figure 3. Classification of solutions of Eqn (8) for $N > 0$.

It follows from the definition of these points that A-points are grouped near the origin of coordinates, whereas B-points are located farther from the origin. Note that the interference maxima corresponding to the A-points are solutions of Eqn (8) only for $m \leqslant 0$, the number of A-points being limited for $N \geqslant 0$ and unlimited for $N < 0$. The maxima corresponding to the B-points may be solutions both for $m \leqslant 0$ and for $m > 0$. In the former case, the number of B-points is limited and is equal to the number of A-points. In the latter case, the number of B-points is not limited. For the sake of brevity, the maxima defined by the A- and B-points will be called the A- and B-maxima, respectively.

Thus, only four types of interference patterns (I – IV) can exist for gas-flow channels of NPLs (see Table 1). Note that for the zeroth line, an interference pattern of type IV can be observed only for a very slight heating of the medium. For type-I interference pattern, each A-maximum should correspond to the B-maximum having the same number m. In experiments for $N \neq 0$, it is not always clear beforehand whether the interference pattern will be of type I or II. Moreover, the maxima corresponding to $m > 0$ (or even all the B-points) may not be observed for a type-I pattern due to a finite length of the channel and a limited size of the interference pattern along the x axis.

To calculate ΔT^* from expression (8), we must assign a corresponding number to each maximum. This problem is solved by using qualitative information on the energy deposition distribution in gas-flow channels of an NPL. Our

Table 1. Types of interference patterns for gas-flow channels of an NPL.

Number of maximum	Type I ($N > 0$)	Type II ($N > 0$)	Type III ($N \leqslant 0$)	Type IV ($N = 0$)
$m \leqslant 0$	A, B	–	A	–
$m > 0$	B	B	–	–

study shows that in the NPL cells with plane uranium layers, the energy deposition near the channel walls is higher than at the centre [18 – 20]. For this reason, the A-maxima near the channel walls are bent towards the channel inlet, while the B-maxima are bent away from the inlet. Fig. 4 shows the interference patterns of types I – III. Calculations were made by putting $\varphi_0 = 0$.

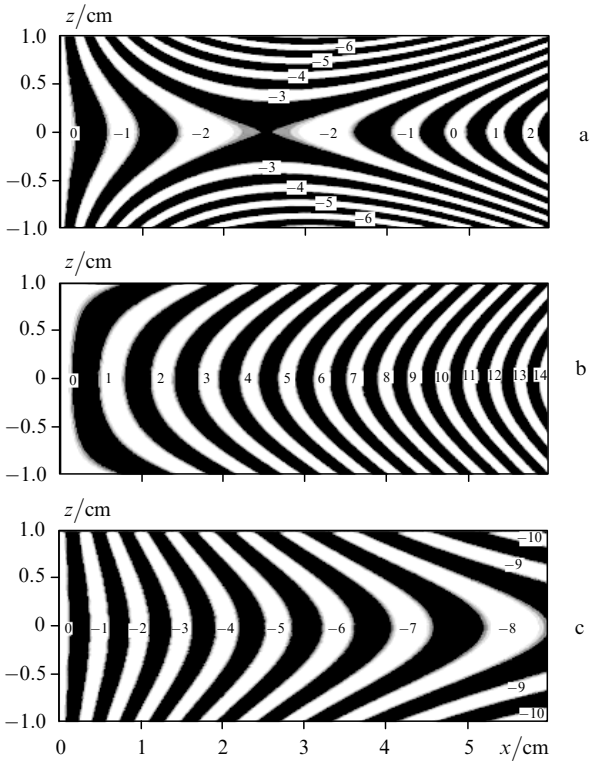

Figure 4. Interference patterns of type I (a), type II (b) and type III (c)

We shall now describe the procedure for assigning a corresponding number to the interference maxima. First, we should determine the type of the interference pattern. For $N \leqslant 0$, interference of type III occurs and the entire volume of the channel is filled with A-maxima. If A-maxima are observed at the channel inlet for $N > 0$, it means that we are dealing with interference of type I. For type-II interference, the whole channel is filled with B-maxima.

Let us now enumerate the maxima. If one of the maxima coincides with the straight line $x = 0$, it is assigned the number $m = 0$ (this case corresponds to $\varphi_0 = 0$). For type-II interference, the first maximum that does not coincide with the straight line $x = 0$ is assigned the number $m = 1$, and the rest of the maxima are enumerated in the ascending order: $m = 2, 3, 4, \ldots$ (Fig. 4b). For an interference pattern of type III, the first maximum has the number $m = 0$, and the following maxima are enumerated in the descending order: $m = -1, -2, -3, \ldots$ (Fig. 4c). The A-maxima for a type-I interference pattern are enumerated in the same way as for

type-III interference, and the B-maxima are enumerated as for type-II interference, the first B-maximum having the same number as the last A-maximum (Fig. 4a). Such a procedure allows us to conclude that the interference patterns presented in Refs [7, 8] are of type I.

For type-I interference, a replacement of the A-maxima by the B-maxima leads to a saddle-like pattern. Some of the A- and B-maxima belong to the same branch, but the A-maxima always dominate the left half of this branch, whereas the B-maxima dominate the right half. The branches are separated at the saddle point, and each type of the maximum determines its own branch (Fig. 4a).

4. Results of calculations

To illustrate the method described above, we analyse the interferogram (Fig. 5a) obtained on the gas-flow prototype in experiments [7, 8]. Helium under a pressure of 2 atm was chosen as the working medium, and the gas flow rate was 8 m s^{-1}. The surface density (thickness) of the oxide layer of ^{235}U was 2.8 mg cm^{-2}. The prototype was irradiated by a pulsed flux of thermal neutrons with a pulse duration of ~ 3 ms at the half-maximum. The flux density of neutrons averaged over the active length of the laser cell was 2.2×10^{15} neutrons cm^{-2} s^{-1} at the pulse maximum. The optical inhomogeneities were measured using a Mach–Zehnder interferometer at the wavelength 0.63 μm of a He–Ne laser. The interferogram in Fig. 5a corresponds to the instant of termination of the neutron pulse, i.e., to the maximum heating of the medium.

The analysis shows that the interferogram pattern presented in Fig. 5 is of type I with $\varphi_0 \approx 4.5$ and $N = 5.25$ cm^{-1}. After enumerating the interference fringes (Fig. 5a), the values of $\Delta T^*(x_m, z)$ were obtained from expression (8), where $z = 0, \pm 2, \pm 4, ..., \pm 10$ mm (the values of ΔT^* for $z = \pm 10$ mm were determined by continuing the interference fringes to the channel walls). The error in determining the temperature is given by the formula

$$\frac{\delta T}{T} \approx \frac{\lambda N}{(n_0 - 1)L} \delta x, \tag{10}$$

where δx is the error in determining the coordinate. For the above-mentioned conditions, we have $\delta T/T \approx 9 \times 10^{-3} N \times \delta x$. Because the error in coordinate measurement is about 0.2 mm (i.e., 1/10 of a fringe), the error in determining the temperature does not exceed 0.3–0.5°C.

The distribution of ΔT^* with an error not exceeding 7 % for $0 < x < 2$ cm and 3 % for $2 < x < 6$ cm can be approximated by the function

$$\frac{\Delta T^*}{T_0} = c_1 \left(1 + c_2 \frac{z^2}{d^2}\right) \left\{1 - \exp\left[-c_3 \left(1 + c_4 \frac{|z^3|}{d^3}\right) \frac{x}{b}\right]\right\}, \tag{11}$$

where $d = h/2 = 1$ cm; $c_1 = 0.141$; $c_2 = 0.177$; $c_3 = 3.502$; $c_4 = 0.712$. Fig. 5b shows the results of approximation using formula (11). Fig. 5c shows the constant-energy lines for the energy density per unit volume $Q^* = c_p \rho \Delta T^*$ supplied to the gas. The maximum energy density per unit volume at the channel axis ($z = 0$) is about of 0.063 J cm^{-3}, in good agreement with the value 0.067 J cm^{-3} given in Ref. [7].

In the output plane, the energy density per unit volume at the channel wall is 1.25 times the value at the channel axis

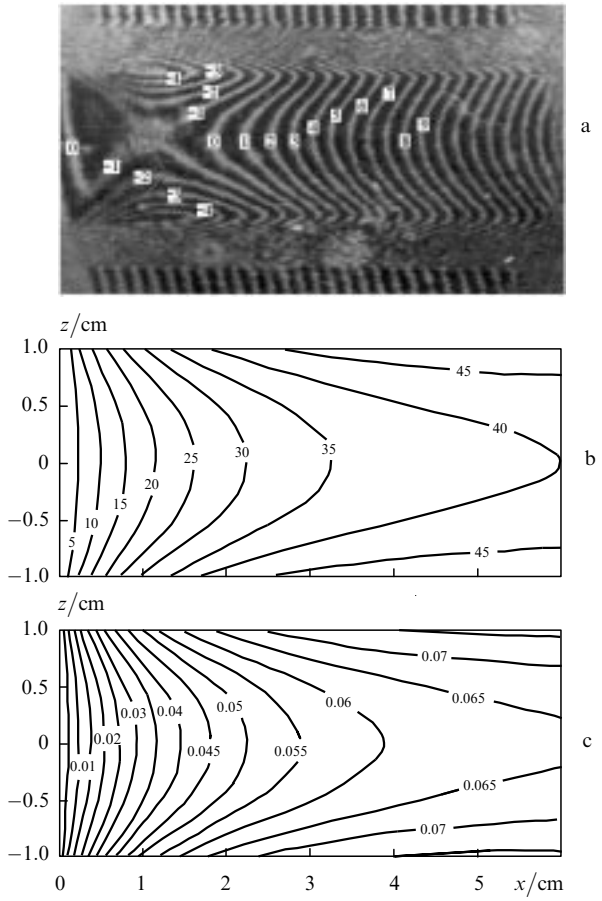

Figure 5. Interferogram for the gas-flow channel under a helium pressure of 2 atm and the gas flow rate 8 m s^{-1} (a), and results of its analysis: temperature distribution ΔT^* (in °C) (b), and the density per unit volume Q^* of the energy deposited in the gas (in J cm^{-3}) (c).

($z = 0$). One can see from Fig. 5b that the temperature at the channel inlet increases rapidly (in the first half of the channel in the direction of the gas flow), and then its growth becomes insignificant. This means that the heating process is nonsteady: the expansion of the gas leads to a flow deceleration for $0 < x < 3$ cm and an acceleration in the region $3 < x < 6$ cm. This is due to the fact that the characteristic time of a neutron pulse is 3 ms, whereas the gas flow time $\tau \approx b/U_0$ is approximately 7.5 ms. Hence, the flow in the case under consideration is essentially nonsteady, and the energy deposition q cannot be determined from expression (2).

Note that the errors associated with the bending of trajectories of beams (refraction) in the measuring channel were not taken into account in the above analysis. The shift of an interference fringe can be determined approximately from expressions

$$\Delta x \approx \frac{n'_x}{n_0} \frac{L^2}{2}, \quad \Delta z \approx \frac{n'_z}{n_0} \frac{L^2}{2}, \tag{12}$$

where n'_x and n'_z are the derivatives of the refractive index n with respect to coordinates x and z.

The maximal shift of the fringe $\Delta x \approx 0.5$ mm is achieved at the channel inlet for $0 < x < 2$ cm; for $2 < x < 6$ cm, we have $\Delta x < 0.2$ mm, which is within the error of measurement of distances on the interferogram. The maximal shift

$\Delta z \approx 0.2$ mm is observed near the cell walls for 1 cm $< x <$ 3 cm. Thus, a considerable distortion (about $\sim 5\,\% - 10\,\%$) of the temperature distribution is observed only at the channel inlet for $0 < x < 2$ cm.

5. Conclusions

In this work, we have presented a technique for analysing the results of interferometric measurements in the gas-flow channels of NPLs. This technique is applicable both for steady-state gas flows and for nonsteady heating of the active medium. It is shown that the gas flowing through the channel makes it possible to use the interferometric technique for determining the gas temperature and the energy deposited in it. The results of analysis of an interferogram obtained in experiments [7, 8] with He under a pressure of 2 atm and a gas flow rate of 8 m s^{-1} are presented. The distribution of the temperature and the energy deposited in the gas over the channel cross section are determined.

Acknowledgements. The author thanks V V Borovkov for useful discussions and B V Lazhintsev for kindly providing the results of his experiments.

References

1. Sinyanskii A A, Melnikov S P *Proc. SPIE Int. Soc. Opt. Eng.* **3686** 43 (1998).
2. Torczynski J R, Gross R J, Hays G N, et al. *Nuclear Sci. Eng.* **101** 280 (1989)
3. Anuchin M G, Grebenkin K F, Kryzhanovskii, Magda E P *Pis'ma Zh. Tekh. Fiz.* **18** (5) 92 (1992).
4. Androsenko A A, Androsenko P A, Gusev N V, D'yachenko P P *Trudy konferentsii 'Fizika Yaderno-Vozbuzhdennoi Plazmy i Problemy Lazerov s Yadernoi Nakachkoi'* (Proceedings of the Conference on the Physics of Nuclear-Induced Plasma and Problems of Nuclear-Pumped Lasers) (Obninsk, 1993) vol. 2, p. 23
5. Vlokh G V, Konak A I, Mat'ev V Yu, et al. *Trudy konferentsii 'Fizika Yaderno-Vozbuzhdennoi Plazmy i Problemy Lazerov s Yadernoi Nakachkoi'* (Proceedings of the Conference on the Physics of Nuclear-Induced Plasma and Problems of Nuclear-Pumped Lasers) (Obninsk, 1993) vol. 2, p. 55
6. Borovkov V V, Lazhintsev B V, Mel'nikov S V, et al. *Izv. Akad. Nauk SSSR, ser. Fiz.* **54** 2009 (1990).
7. Borovkov V V, Lazhintsev B V, Mel'nikov S V, et al. *Kvantovaya Elektron* **22** 1187 (1995) [*Quantum Electron.* **25** 1149 (1995)]
8. Borovkov V V, Lazhintsev B V, Mel'nikov S V, et al. *Trudy II Mezhdunarodnoi Konferentsii 'Fizika Yaderno-Vozbuzhdennoi Plazmy i Problemy Lazerov s Yadernoi Nakachkoi'* (Proceedings of II International Conference on the Physics of Nuclear-Induced Plasma and Problems of Nuclear-Pumped Lasers) (Arzamas-16, 1995), vol. 1, p. 399
9. Bogdanov V N, Vasilenko A G, Zherebtsov V V, et al. *Trudy II Mezhdunarodnoi Konferentsii 'Fizika Yaderno-Vozbuzhdennoi Plazmy i Problemy Lazerov s Yadernoi Nakachkoi'* (Proceedings of II International Conference on the Physics of Nuclear-Induced Plasma and Problems of Nuclear-Pumped Lasers) (Arzamas-16, 1995), vol. 2, p. 172
10. Kolesov V F in: *Dinamika Yadernikh Reaktorov* (Dynamics of Nuclear Reactors), Ed. By Ya I Shevelev (Moscow: Energoatomizdat, 1990)
11. Landau L D, Lifshits E M *Gidrodinamika* (Hydrodynamics) (Moscow: Nauka, 1988)
12. Loitsyanskii L G *Mekhanika Zhidkosti i Gaza* (Mechanics of Fluids and Gases) (Moscow: Nauka, 1973)
13. Born M, Wolf E *Principles of Optics*, 4th ed. (Oxford: Pergamon Press, 1969; Moscow: Mir, 1970)
14. Landsberg G S *Optika* (Optics) (Moscow: Nauka, 1976)
15. Babadei M S, Bogdnov V N, Vlokh G V, Dzyatko Yu N, et al. *Trudy II Mezhdunarodnoi Konferentsii 'Fizika Yaderno-Vozbuzhdennoi Plazmy i Problemy Lazerov s Yadernoi Nakachkoi'* (Proceedings of II International Conference on the Physics of Nuclear-Induced Plasma and Problems of Nuclear-Pumped Lasers) (Arzamas-16, 1995), vol. 2, p. 154
16. Kolmogorov A N, Fomin S V *Elementy Teorii Funktsii i Funktsional'nogo Analiza* (Elements of the Theory of Functions and Functional Analysis) (Moscow, Nauka, 1989)
17. Mat'ev V Yu, Sizov A N, et al. *Trudy II Mezhdunarodnoi Konferentsii 'Fizika Yaderno-Vozbuzhdennoi Plazmy i Problemy Lazerov s Yadernoi Nakachkoi'* (Proceedings of the Conference on the Physics of Nuclear-Induced Plasma and Problems of Nuclear-Pumped Lasers) (Arzamas-16, 1995), vol. 1, p. 407
18. Mat'ev V Yu *Trudy Konferentsii 'Fizika Yaderno-Vozbuzhdennoi Plazmy i Problemy Lazerov s Yadernoi Nakachkoi'* (Proceedings of the Conference on the Physics of Nuclear-Induced Plasma and Problems of Nuclear-Pumped Lasers) (Obninsk, 1993), vol. 2, p. 79
19. Mat'ev V Yu, Sizov A N *Trudy Konferentsii 'Fizika Yaderno-Vozbuzhdennoi Plazmy i Problemy Lazerov s Yadernoi Nakachkoi'* (Proceedings of the Conference on the Physics of Nuclear-Induced Plasma and Problems of Nuclear-Pumped Lasers) (Obninsk, 1993), vol. 2, p. 209
20. Torczynski J R *J. Thermophys. Heat Transfer* **5** 318 (1991)